Ocean Dynamics
October 2014, Volume 64 Issue 10 Pages 1499-1516
https://doi.org/10.1007/s10236-014-0754-1
https://archimer.ifremer.fr/doc/00216/32733/

Modelling the effects of *Zostera noltei* meadows on sediment dynamics: application to the Arcachon lagoon

Kombiadou Katerini [1, 2, *] , Ganthy Florian [1, 2], Verney Romaric [1], Plus Martin [2], Sottolichio Aldo [3]

[1] IFREMER, DYNECO PHYSED, F-29280 Plouzane, France.
[2] IFREMER, LER AR, F-33120 Quai Commandant Silhouet, Arcachon, France.
[3] Univ Bordeaux, CNRS, UMR EPOC 5805, F-33615 Pessac, France.

* Corresponding author : Katerina Komabiadou, email address : kobiadou@civil.auth.gr

Florian.Ganthy@ifremer.fr ; romaric.verney@ifremer.fr ; Martin.Plus@ifremer.fr ; a.sottolichio@epoc.u-bordeaux1.fr

Abstract :

A three-dimensional model has been modified to describe the complex interactions between hydrodynamics, sediment dynamics and biological parameters in the presence of Zostera noltei. The model treats seagrass leafs as flexible blades that bend under hydrodynamic forcing and alter the local momentum and turbulence fluxes and, therefore, the benthic shear conditions; these changes cause related changes to the mass balance at the boundary of the bed, in turn affecting the suspended matter in the column and ultimately primary productivity and the growth of the dwarf-grass. Modelling parameters related to the impact of Z. noltei to the local flow and to erosion and deposition rates were calibrated using flume experimental measurements; results from the calibration of the model are presented and discussed. The coupled model is applied in the Arcachon Bay, an area with high environmental significance and large abundance of dwarf-grass meadows. In the present paper, results from preliminary applications of the model are presented and discussed; the effectiveness of the coupled model is assessed comparing modelling results with available field measurements of suspended sediment concentrations and seagrass growth parameters. The model generally reproduces sediment dynamics and dwarf-grass seasonal growth in the domain efficiently. Investigations regarding the effects of the vegetation to the near-bed hydrodynamics and to the sediment suspension in the domain show that dwarf-grass meadows play an important part to velocity attenuation and to sediment stabilisation, with flow and suspended sediment concentrations damping, compared to an unvegetated state, to reach 35-50 and 65 %, respectively, at peak seagrass growth.

Keywords : Zostera noltei, Sedimentation, Erosion, Arcachon lagoon, Intertidal mudflats, Flume measurements

1. Introduction

The high environmental significance of vegetated beds has drawn scientific interest to the study of the flow and/or ecosystem dynamics in their presence over the last decades. It is a well documented fact that the existence of aquatic vegetation has a strong impact on local hydrodynamics as well as on the transport and deposition of sediments (e.g. Gacia et al. 1999). The interaction between seagrasses and flow results in reduced flow velocities near the bed and, therefore, in reduced shear conditions that could favour deposition and decrease resuspension of newly deposited matter (Ackerman and Okubo 1993; Gacia et al. 1999; Neumeier and Amos 2006). However, the increase of turbulence near the interface between the canopy and the unrestricted flow and the development of instabilities may lead to intense mixing and, therefore, could affect the local deposition rates. At the same time, the leaf blades bend under hydrodynamic forcing, thus changing the local balance of forces, and producing a canopying effect; this effect could prevent particles from settling through the leaves and deposited particles from resuspending, while the rhizome and root system of the plants act as a stabilizing agent against erosion (Bouma et al. 2005b; Bouma et al. 2009; Dauby et al. 1995; Gacia et al. 1999). Small-scale localised scour has also been identified around the shoots in cases of low density canopies (Lefebvre et al. 2010). At the same time, the vegetation type (shoot stiffness, diameter and length) significantly affects flow conditions; Gacia et al. (1999) report velocity attenuation of 14-67% for *Posidonia oceanica* from insitu measurements, while Gambi et al. (1990) measured attenuation of the order of 50-90% inside the canopy from flume experiments using *Zostera marina*. It, thus, becomes evident that the local sediment balance is highly complex and dependant on the vegetation type and density.

The effects of vegetated beds on local hydrodynamics has been investigated for different types of aquatic plants by in situ measurements (Gacia et al. 1999; Bouma et al. 2005a; Temmerman et al. 2005) and flume experiments using natural (Grizzle et al. 1996; Bouma et al. 2005b; Lefebvre et al. 2010) or artificial vegetation (Nepf and Vivoni 2000; Lopez and Garcia 2001; Ghisalberti and Nepf 2002; Fonseca and Koehl 2006; Nepf and Ghisalberti 2008; Bouma et al. 2009). Three distinct areas have been identified in vegetated flows: a low-velocity area within the canopy, a transition zone of increased shear at the interface and a free-stream velocity layer above the canopy (Lefebvre et al. 2010). The penetration of shear-scale turbulence into the canopy is limited by the canopy drag, while a mixed layer can form at the interface between restricted and unrestricted flow, leading to the formation of Kelvin-Helmholtz instabilities and coherent vortices within the mixing layer (Ghisalberti and Nepf 2002). A turbulence maximum is generally found at the water-canopy interface (Gambi et al. 1990; Ghisalberti and Nepf 2002; Lefebvre et al. 2010). Upstream of the canopy, the flow adjusts over a length scale proportional to the canopy width, while the length scale of the interior adjustment region depends on the canopy flow-blockage (Rominger and Nepf 2011). Regarding the flow of emergent and submerged canopies, the velocity profile is determined by the

variation in vegetative drag for the case of emergent vegetation, whereas once a canopy becomes submerged, the vertical penetration of turbulent stress defines a vertical exchange zone (Nepf and Vivoni 2000).

There are generally two different approaches to model the velocity profile through and above submerged vegetation: a two-layer approach, which separately describes the flow in the vegetation layer and in the upper layer (Righetti and Armanini 2002; Defina and Bixio 2005; Rominger and Nepf 2011), and a modified turbulence modelling approach, in which the drag due to vegetation is taken into account not only in the momentum equation but also in the turbulence closure scheme (Fischer-Antze et al. 2001; Lopez and Garcia 2001; Temmerman et al. 2005). It must be noted that stiff and bending canopies present different effects on the hydrodynamics (Ghisalberti and Nepf 2009). Backhaus and Verduin (2008) developed a Lagrangian plant model to simulate the movement of plants under oscillatory flow at small scales. Few large-scale, three-dimensional modelling applications for the investigation of the hydro-sedimentary effects of the presence of vegetated beds have also been implemented. Temmerman et al. (2005) formulated a model for the three-dimensional effects of vegetation on the flow, combined to a sediment transport model; their results advocate that vegetation has a pronounce impact on flow routing and on the spatial sedimentation patterns. Verduin and Backhaus (2000) applied a coupled three-dimensional hydrodynamic model with a 10-layer canopy model for the description of the flow above and within an *Amphibolis antarctica* meadow. Milbradt and Schonert (2008) developed an object-oriented holistic framework for ecohydraulic simulation of vegetated flows based on a fuzzy logic rule-based system and applied it to predict seagrass around an island in the North Sea.

It becomes evident that the interactions between seagrasses, flow and sediment pathways are highly complex and that it would be very difficult to extrapolate experimental data to study these phenomena in the scale of a coastal region. In that aim, we focused on the development of a three-way coupled mathematical/process-based model to describe the flow, sediment and biological parameters' dynamics in the bay of Arcachon (SW France). To our knowledge, this is the first attempt to implement a three-dimensional model that simulates all the main controlling parameters of the problem in a fully-coupled way and apply it to a large-scale domain.

The bay of Arcachon (Fig.1) is a triangular-shaped, enclosed, mesotidal environment that consists of an intricate network of main and secondary channels and of the intertidal area that is partly occupied by *Zostera noltei* (seagrass commonly known as dwarf-grass) at depths of 0.3-3.1 m below the lowest astronomical tide. The tide is semi-diurnal and the tidal amplitude varies from 0.8 to 4.6 m (Plus et al. 2010). The sediment is mainly sandy in the channel system and ranges from sand to mud in the intertidal area. The sediment grain sizes range from 17 to 40 μm in the vegetated area of the mudflats, with coarser sediments (~250 μm) in the deep channels. The sorting of the sediment mainly ranges from moderately well to poorly sorted. Seven rivers discharge in the bay, with the two largest (Eyre and Porges) providing

the bulk freshwater (593 and 195 million m^3/year, respectively) and sediment influx (4000 and 1500 t/year, respectively) to the domain. The Bay of Arcachon is an area of high ecological productivity, linked to various socioeconomic activities (oyster-farming, fishing, leisure etc). The population growth in the area is relatively high (42,000–100,000 inhabitants between 1936 and 2000), with around 500,000 visitors a year (Henocque, 2003); the total length of stay for the 2004 tourist period reached 6,612,000 nights (Cholvy, 2008), while for the summer of 2008, more that 12,000 boats (skiffs, sailing boats etc) visited the area (Le Berre et al 2009). Regarding oyster farming and fishing, the total production of marketable oysters reached 7,875 tons in 2010 (Scourzic et al 2011) and the total revenue of the local fishing fleet (315 fishermen, 102 fishing boats) reached 14,690,000,000€ in 2004 (Fabrègues 2005). Apart from its socioeconomic value, the Bay of Arcachon is the area of the largest abundance of *Zostera noltei* in Europe (Auby and Labourg 1996), even though a significant reduction of their coverage has been documented during the last decade; the total surface of dwarf-grass meadows in the Arcachon bay was reduced by 33% between 1989 and 2007, reduction that corresponds to a total loss of 22.8 km^2 (Plus et al. 2010). The reason for this decline is still unclear; several hypotheses have been made, including reduction of light in the water column or burial by fine sediment due to extensive dredging, intense grazing by Brent geese and swans, whose population increased during the period in question, as well as pathogenic reasons (Plus et al. 2010). The most recent (2007) mapping of the *Zostera* meadows in the intertidal area of the Arcachon lagoon reports a vegetated surface of 45.7 km^2 with high (75%) coverage in the western part of the lagoon and lower (25%) in the eastern one (Plus et al. 2010). The corresponding densities of the meadows range from 4000 to 9000 shoots/m^2 (low) during winter and from 11000 to 22000 shoots/m^2 (high) during summer (Auby and Labourg 1996). Ganthy (2011) investigated the impacts of *Zostera noltei* on hydrodynamics and sediment dynamics with extensive laboratory and field experiments. Laboratory experiments (Ganthy 2011) were conducted in a recirculating flume using natural dwarf-grass plants of different seasonal characteristics and included deposition and erosion tests; the recorded velocity profiles and suspended sediment concentrations showed a pronounced impact of the aquatic plants on both the flow and on sediment transport in the flume. A two-year field survey (Ganthy et al. 2013a) was conducted in the intertidal mudflat of the Arcachon lagoon and included continuous monitoring of bed altimetry, tide and wave recordings and monthly sampling and analysis of sediment parameters and meadow characteristics. The survey data showed that in all vegetated stations the bed accreted proportionally to the seasonal growth of the meadows, while during the seasonal degeneration of dwarf-grasses the meadow continued to retain sediment, preventing erosion of the bed.

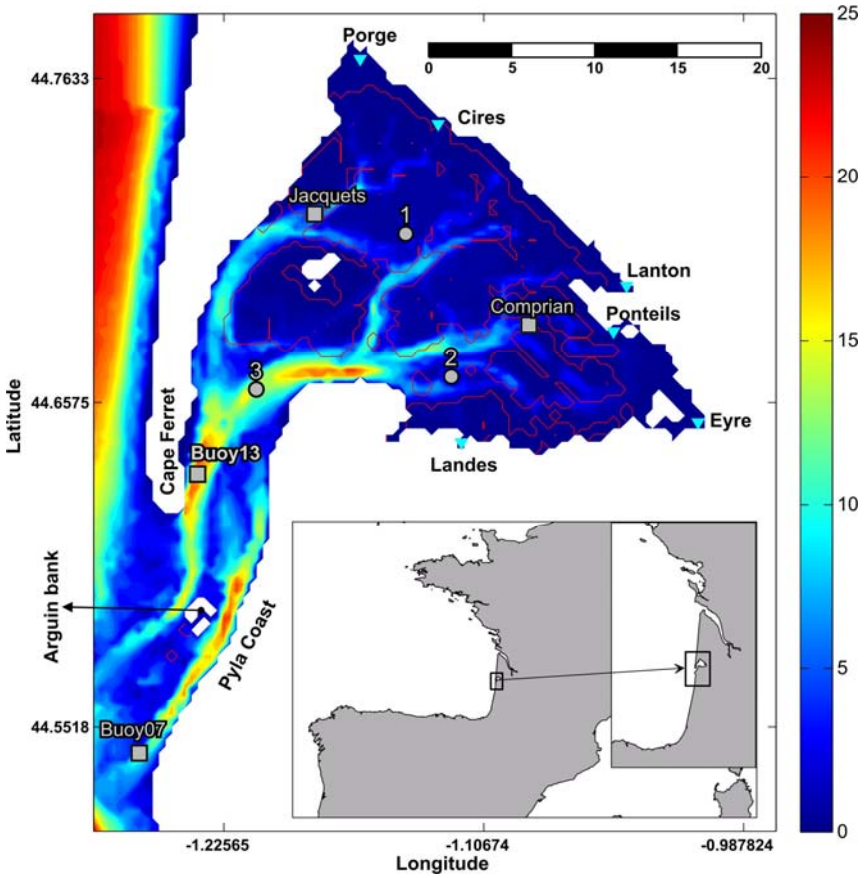

Fig. 1 *Bathymetry of the Arcachon lagoon and location of the area in the map of France; the rivers of the area and selected stations are noted on the map and the scale bar is in km*

Large uncertainties remain on the possible consequences of the decline of *Zostera* meadows in the Arcachon lagoon, both in terms of sediment balance and lagoon morphology, but also in terms of primary production and hence of ecosystem productivity, and interaction/loops between these two compartments of the ecosystem. In order to investigate different scenarios, it was decided to implement a fully coupled 3D numerical model simulating hydrodynamics, sediment dynamics and ecological dynamics, including the main interactions between these three compartments. More specifically, the coupled model describes the growth of the *Zostera noltei* (included in the biogeochemical modules of the model), their impact to the near-bed flow and local deposition and erosion rates, while these changes, in turn, affect the growth of the dwarf-grass themselves; these interactions are graphically depicted in Figure 2. In the following parts of the paper, the term 'coupled model' is used to describe this integrated version of the model that simulates these complex interactions and the interrelationships between *Zostera noltei* populations, local hydrodynamics and sediment dynamics.

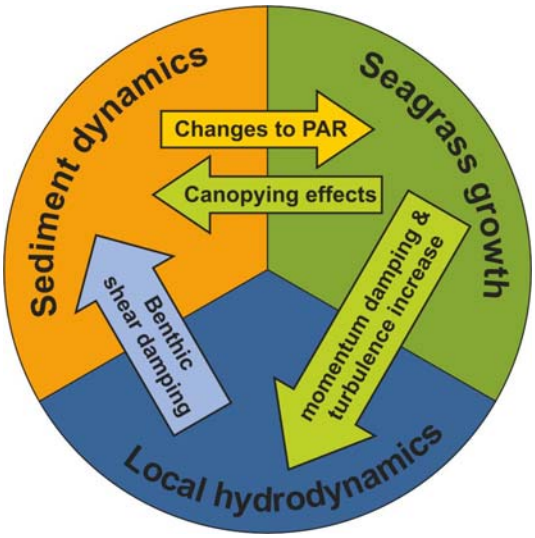

Fig. 2 *Schematic outline of the interaction between the main modelling parameters*

The present paper focuses on the main aspects of the coupled model and the discussion of results from characteristic applications in the Arcachon lagoon with reference to corresponding field measurements. The calibration of the model, so as to express the effect of *Zostera noltei* to the flow and erosion/deposition rates, was performed using flume experimental measurements conducted with natural plants (fully detailed in Ganthy, 2011). Regarding the structure of the paper, these laboratory experiments are briefly presented, followed by the description of the mathematical model. The results of the model presented, include results from the calibration of hydrodynamics and sediment dynamics and several results from preliminary applications of the fully coupled model in the Arcachon lagoon.

2. Flume measurements

The flume experimental measurements were conducted by Ganthy (2011) in the HYDROBIOS flume (Orvain et al. 2003), a recirculating flow system that can generate free-stream velocities up to 0.6m/s, with an accuracy of 0.01m/s; flume features (curved walls and honeycomb grid at the entrance) allow the development of fully turbulent and uniform flow across the test section (width x length: 0.4m x 0.9m) where the sediment and vegetation are introduced. The flume is equipped with an Acoustic Doppler Velocimeter (ADV), mounted on a 3D positioning system for the recording of vertical velocity profiles along the channel. Two profiles were recorded during the experiments, one 0.15m upstream from the sediment patch and the second in the middle of the patch. Each velocity profile recording covered the range between 0.003m and 0.143m from the bed. The optical tubidity meter, located 0.15m downstream from the sediment section, provided suspended sediment concentration recordings.

A survey was conducted in the Arcachon lagoon (SW France) in 2010, during which vegetated sediment cores were collected from the mudflat (location 1 in Fig.1) using rectangular box corers (0.4m x 0.3m x 0.05m) during 5 sampling periods (Ganthy 2010). These samples (T1 to T5), along with a bare sediment core

(Tsed), which serves as a reference case, correspond to the sampling periods of: 16/03 (T1), 30/03 (T2 and Tsed), 13/04 (T3), 27/04 (T4) and 06/09 (T5). The collection of the core samples was conducted so as to assure minimum disruption to the sediment/seagrass sample (Widdows et al. 2008) and they were kept in a stalling container for 12 hours to decrease the presence of bioturbators inside the meadows. Following, the samples were placed in the test section of the flume to form a uniform, nearly undisturbed bed and the flume was filled with oxygenated filtered seawater (salinity 30-31).

Two different sets of experiments (deposition and erosion tests) were conducted for each of the 6 natural sediment samples. The sedimentary parameters and vegetation characteristics for these tests are listed in table 1. In each of the tests, the velocity in the flume was regulated between 0.1 and 0.4m/s, increasing (from 0.1-0.4m/s for deposition) or decreasing (from 0.4-0.1m/s for erosion) in steps of 0.1m/s. Each velocity step lasted 90mins, time during which the conditions in the flume remained stable. These measurements will be used to calibrate the vegetation/hydrodynamics/sediment dynamics interaction formulations on i) hydrodynamics and bed shear stress, ii) sediment processes.

Table 1*. Meadow characteristics and sediment composition (mean values) for the 6 sediment cores; Tsed is the reference cores, without vegetation*

		Tsed	T1	T2	T3	T4	T5
Dwarf-grass characteristics							
Shoot density [m^{-2}]		-	7960	9530	8220	12580	18970
No of leafs/shoot		-	3.35	3.59	5.18	6.43	2.69
Leaf length (h_{leaf}) [mm]		-	56	72	66	63	150
Leaf diameter (φ) [mm]		-	0.6	0.6	0.6	0.8	1.2
Leaf Area Index (LAI)		-	0.85	1.42	1.78	4.22	9.03
Leaf height	$\bar{U}$=0.1m/s	-	35	40	37	55	93
(h_{leaf}) [mm]	$\bar{U}$ =0.2m/s	-	25	35	24	35	73
per velocity	$\bar{U}$ =0.3m/s	-	20	24	22	28	59
step	$\bar{U}$ =0.4m/s	-	15	20	16	20	48
Deposition tests: Initial sediment concentrations in water [kg/m^3]							
Fine fraction		1.75	-	1.58	1.71	1.60	1.80
Coarse fraction		2.05	-	2.81	2.09	2.20	2.38
Total		3.80	4.41	4.39	3.80	3.80	4.18
Erosion tests: Initial sediment dry densities in bed [kg/m^3]							
Fine fraction		247.42	346.09	332.60	353.50	434.52	296.64
Coarse fraction		766.58	559.91	522.41	346.50	330.48	733.36
Total		1014.00	906.00	855.00	700.00	765.00	1030.00

3. Model description

The modelling platform includes the coupling of hydro-sediment dynamics and biogeochemical cycles regarding the effects and growth of *Zostera noltei* (Fig.2). More specifically, the Model for Applications at Regional Scale (MARS) (Lazure and Dumas 2008) was modified to describe the 3-dimensional hydrodynamic response of the flow to the aquatic vegetation. MARS is a thee-dimensional, free surface, sigma coordinate,

hydrodynamic model that solves the primitive equation using a semi-impicit scheme for the barotropic mode. The model enables the description of hydrodynamics from the regional to local scales, as well as the use of various high-level turbulence closure schemes (i.e. κ-ε, κ-ω).

The sediment transport module (fully detailed in Le Hir et al. 2011) describes the main processes that control the transport and near-bed dynamics of both cohesive and non cohesive sediments, i.e sediment settling and deposition (including flocculation processes through parameterized formulations), and mixed sediment erosion (hybrid formulation for sand/mud mixtures based on the Partheniades equation). Two classes of sediment are used (one mud, one sand, representative of the sediment distribution on the whole lagoon). It is noted that the model calculates the erosion flux of bare sediment using the Partheniades formulation that takes into account an erosion rate and the excess shear stress (over the critical erosion threshold). The erosion rate and the critical shear stress values are defined for the case of mixed sediments. Depending on the sediment composition, the bed can be classified as pure sand (mud content below a critical value, i.e. 0.2), pure mud (mud content over a critical value, i.e. 0.7) or as a sand-mud mixture. In the first case the critical shear stress is defined by the sand diameter, in the second one using a power law of the mud concentration (Eq. 12). In the third case (mixed sediment) the critical shear threshold is defined taking into account the percentages of mud and sand in the sediment and interpolating linearly between the corresponding values for these classes (calculated as mentioned above). A similar approach is used for the determination of the erosion rate.

The critical shear stress for erosion of sand-mud mixture is calculated interpolating the corresponding values of the two constituents with respect to the content of each sediment class. Sediments are deposited in thin layers, which can be eroded by tidal currents. In this preliminary step, wave forcing and bed consolidation effect are not accounted for.

The biogeochemical model (Guillaud et al. 2000, Huret et al. 2013), describes the planktonic food chain (photosynthesis, respiration, grazing, excretion, etc.), nitrogen, phosphorus and silicon cycling (mineralization processes and fluxes at the water–sediment interface), coupled with a module that describes the growth of *Zostera noltei* seagrasses (adapted from Plus et al. 2003). Seven state variables represent the macrophytes: the above and below-ground biomass, the density of shoots per square meters and the above and the below-ground nitrogen and phosphorus pools. Contrary to the phytoplancton, whose growth relies on nutrients available in the water column (in addition to the PAR and the water temperature), *Zostera noltei* can uptake nutrients by their rhizomes and roots in sediment interstitial waters as well as from their leaves in the water column. Moreover, due to their higher tissue content in cellulose, seagrass biomass is less labile than other organic detritus coming from plankton decay and is, thus, more inclined to be exported outside the lagoonal system.

The model parameters were calibrated and validated using laboratory flume experiments, with good correlation between measured and simulated hydrodynamics (Ganthy 2011; Ganthy et al. 2013b).

Information regarding the growth and characteristics of the *Zostera noltei* meadows in the domain are provided by the biogeochemical modules, while the primary productivity and the growth of the dwarf-grasses are in turn highly affected by the changes to local hydrodynamics and suspended sediment concentrations (attenuation of photosynthetically active radiations, PAR). At the same time, the effects of aquatic vegetation to the sediment dynamics were taken into account both directly, through the calibrated values of settling and sediment erodibility parameters, and indirectly, through the changes to the benthic shear by the corresponding changes to the near-bed hydrodynamics caused by the presence of leaf blades.

Following we describe how MARS3D modules (hydrodynamics, sediment transport and biogeochemical modules) were newly modified to describe the interaction between the presence of aquatic vegetation and the main physical processes (hydrodynamics and erosion/deposition processes).

3.1 Hydrodynamics and vegetation

The hydrodynamics module was modified to describe the 3-dimensional hydrodynamic response of the flow to the aquatic vegetation, taking into account the loss of momentum due to drag exerted on the blades, the increase in turbulence and the bending of the leaves under forcing. Drag resistance was included as an additional friction force, while the production and dissipation of turbulent kinetic energy due to the restricted flow were included in the κ-ε turbulence closure scheme (Temmerman et al. 2005; Ganthy 2011; Ganthy et al., 2013b).

Plant leafs are described as flexible cylindrical elements that deform under hydrodynamic shear and also exert drag force to the flow and change the turbulent scales.

The drag due to the presence of the cylindrical obstructions is taken into account as a momentum loss term:

$$F(z) = -\frac{1}{2}\cdot C_D \cdot \rho \cdot \phi(z) \cdot n(z) \cdot |u(z)| \cdot u(z) \qquad (1)$$

In the above equation C_D is the drag coefficient for the vegetated case (set at 1.5), φ(z) and n(z) are the diameter and number of plant elements per unit area al level z, ρ is the seawater density and u(z) the horizontal flow velocity.

The changes to turbulent kinetic energy production (k) and dissipation (ε), due to the presence of the seagrass leafs, are expressed using additional source terms:

$$\left(\frac{\partial k}{\partial t}\right)_{veg} = \frac{1}{1-A(z)}\cdot\frac{\partial}{\partial z}\left\{\left(1-A(z)\right)\cdot\frac{\nu+\nu_t}{\sigma_k}\cdot\frac{\partial k}{\partial z}\right\} + T(z) \qquad (2)$$

$$\left(\frac{\partial \varepsilon}{\partial t}\right)_{veg} = \frac{1}{1-A(z)}\cdot\frac{\partial}{\partial z}\left\{\left(1-A(z)\right)\cdot\frac{\nu+\nu_t}{\sigma_\varepsilon}\cdot\frac{\partial \varepsilon}{\partial z}\right\} + T(z)\cdot\tau_\varepsilon^{-1} \qquad (3)$$

where ν and ν_t are molecular and eddy viscosities; σ_k and σ_ε are turbulent Prandtl-Schmidt numbers for self mixing turbulence and small scale vorticity, respectively (σ_k=1.0 and σ_ε=1.3). A(z) is the cross-sectional plant

area per unit area at the level z, T(z) is the work spent by the fluid and τ_ε is the energy dissipation timescale, which equals the minimum of the corresponding values for free turbulence and for plant-restricted eddies:

$$A(z) = {\pi \cdot \phi(z)^2}/{4} \cdot n(z) \quad (4)$$

$$T(z) = F(z) \cdot \frac{u(z)}{\rho} \quad (5)$$

$$\tau_\varepsilon = \min\left[\frac{1}{c_{2\varepsilon}} \cdot \left(\frac{k}{\varepsilon}\right), \frac{1}{c_{2\varepsilon} \cdot \sqrt{c_\mu}} \cdot \left(\frac{L(z)^2}{T(z)} \right)^{1/3} \right] \quad , L(z) = c_{lz} \sqrt{\frac{1 - A(z)}{n(z)}} \quad (6)$$

L(z) is the typical eddy size limited by the minimum distance between plant elements and the coefficients $c_{2\varepsilon}$, c_μ and c_{lz} have been set to 1.96, 0.09 and 0.3, respectively.

The height of the bent canopy (H_C in mm) is predicted from the depth-averaged velocity ($\bar{U}$ in cm/s) and the LAI by the following formula that is fitted to the laboratory data (Ganthy 2011):

$$h_{can} = 46.57 - 1.58 \cdot \bar{U} + 2.62 \cdot LAI - 0.11 \cdot \bar{U} \cdot LAI + 0.02 \cdot \bar{U}^2 + 0.48 \cdot LAI^2 \quad (7)$$

3.2 Sediment transport and vegetation

The sediment balance at the seabed boundary is the result of the equilibrium between deposition (S_D) and erosion (S_E) fluxes (Le Hir et al. 2011):

$$S_E - S_D = \underbrace{\varepsilon_s \left(\tau_b - \tau_{cr,e} \right)}_{\text{erosion flux}} - \underbrace{w_s c \left(1 - \frac{\tau_b}{\tau_{cr,d}} \right)}_{\text{deposition flux}} \quad (8)$$

In the equation ε_s is the erosion rate, w_s is the sediment settling velocity, c is the suspended sediment concentration near the bed, τ_b is the shear stress at the bed and $\tau_{cr,e}$ and $\tau_{cr,d}$ are the corresponding critical values for erosion and deposition, respectively. It must be noted that no deposition (S_D=0) takes place when the shear stress is higher than the critical threshold for deposition ($\tau_b > \tau_{cr,d}$) and, similarly, no erosion (S_E=0) takes place when the shear stress is lower than the critical threshold for erosion ($\tau_b < \tau_{cr,e}$). The critical shear stress for erosion of sand-mud mixture is calculated interpolating the corresponding values of the two constituents with respect to the content of each sediment class.

3.2.1 Bed shear stress

In cases of turbulent and fully rough bottom boundary layer the shear stress conditions are described by the law-of-the-wall:

$$U(z) = \frac{u_*}{\kappa} \ln\left(\frac{z}{z_0} \right), \qquad \tau_b = \rho \cdot u_*^2 \quad (9)$$

Where u_* is the shear stress velocity, κ the von Karman constant (κ=0.4), z is the distance from the bed, z_0 the roughness length and τ_b the bottom shear stress. For the correct representation of the sediment deposition/erosion fluxes it is important to simulate the bottom shear stress as accurately as possible. In that aim, and taking into account that the presence of the canopy changes (increases) the roughness in the

area of the bed (Gacia et al. 1999; Lefebvre et al. 2010; Ganthy et al 2013b), the sediment roughness length (z_0) was related to the Leaf Area Index (LAI) of the canopy, which equals the total leaf area per vegetated (ground) area [m^2/m^2] through a logarithmic relationship of the form:

$$z_0 = \max\left(z_{0(bs)}, \xi_1 \cdot \ln\left(\frac{LAI}{\xi_2}\right)\right) \quad (10)$$

The optimum correlation of simulated and measured (flume experiments) near-bed shear conditions (R^2=0.81) is given in Figure 3, which was obtained for ξ_1=0.0014 and ξ_2=0.3 and a minimum roughness length for bare sediment $z_{0(bs)}$=0.2 mm. The roughness length in the vegetated bed ranges from 0.15 to 0.48cm, which is well within the range reported by Lefebre et al. (2010), who calculated z_0 values between 0.002 and 0.547cm from laboratory experiments using natural *Zostera marina* plants and densities between 300 and 750shoots/m^2.

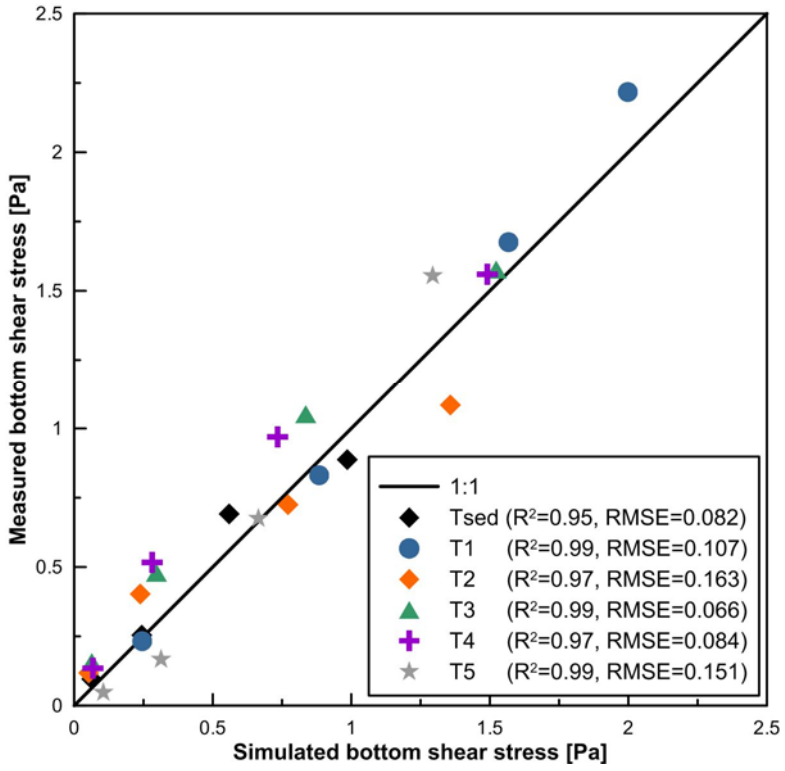

Fig. 3 *Correlation of simulated and laboratory benthic shear stress [Pa]. The correlation coefficients (R^2) and Root Mean Square Errors (RMSE in Pa) are noted on the legend*

3.2.2 Sediment deposition

Six flume experiments were conducted (1 test with bare sediment, 5 tests with natural *Zostera noltei*) to investigate the influence of vegetation on deposition processes, monitoring the SSC time evolution during decreasing flow velocities steps. A pre-estimation of the expected final settling velocities was made using the deposition fluxes and the concentrations observed in the experiments. Applying this estimated value to a simplified deposition model produced an evolution of the concentration with time for the bare sediment case that was generally close to the experimental measurements. Using the same formulation for all tests,

thus ignoring any effect of vegetation on deposition fluxes, we observed that the settling velocities are underestimated in all vegetated cases. This suggests that the seagrass leafs physically interfere with deposition, through particle-leaves collision, for example.

From our calculations and the observations made by Ganthy (2011), it follows that the LAI and the height of the bent canopy play an important part to the deposition rates in the vegetated areas of the flume. More specifically, the deposition rates generally increase with the density of the meadow (increasing LAI values) and the bending of the canopy leafs (increasing shear) up to a 'critical' value, after which the deposition rates decrease. The latter is observed in highly dense and bent canopies, where leafs form a physical 'barrier' to sediment that try to settle through them, thus reducing deposition fluxes. Our estimation is in agreement with the findings of Gacia et al. (1999) and Ganthy et al (2013a), who also found the relationship between LAI and deposition fluxes to be nonlinear, with a significantly reduced sedimentary flux at high LAIs. This behaviour is schematically described in Figure 4.

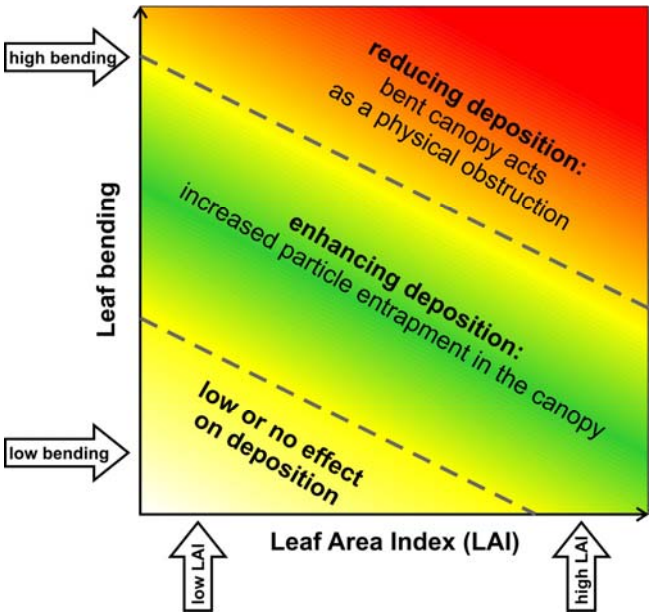

Fig. 4 *Schematic representation of the direct impacts of leaf bending and LAI on the deposition rates*

These direct effects of the meadow characteristics to the settling fluxes need to be accounted for by the model; we, thus, modified the calculation of the setting velocity of sediments in the vegetated area of the flume (inside the canopy) to express the direct effects of seagrass leafs to the sediment settling rate (w_s), using the non dimensional LAI:

$$w_s = w_{s0} \cdot \frac{h_{can}}{h_{leaf}} \cdot 2\exp\left[-\frac{(LAI - LAI0)^2}{LAI0^4} \right] \quad (11)$$

In the above equation w_{s0} is the initial settling velocity (for unvegetated bed), h_{can} and h_{leaf} are the canopy and unbent leaf height and LAI. Essentially, the h_{can}/h_{leaf} ratio expresses leaf bending and LAI the thickness of the canopy. The constant parameter LAI0 represents the LAI of the meadow that induces the strongest enhancement to the settling velocity. LAI0 was estimated at 4, based on the best fit of the simulated

deposition experiments to the flume data (presented in the following section); it is noted that a non-linear relationship between LAI and deposition fluxes is also reported by Gacia et al. (1999), who measured peak sedimentation fluxes at LAI of around 2.5 for *Posidonia oceanica*. The variation of the enhancement ($w_s/w_{s0}>1$) or reduction ($w_s/w_{s0}<1$) of settling rates with the bending ratio from the 5 vegetated deposition test, predicted by equation 11, is presented in figure 5.

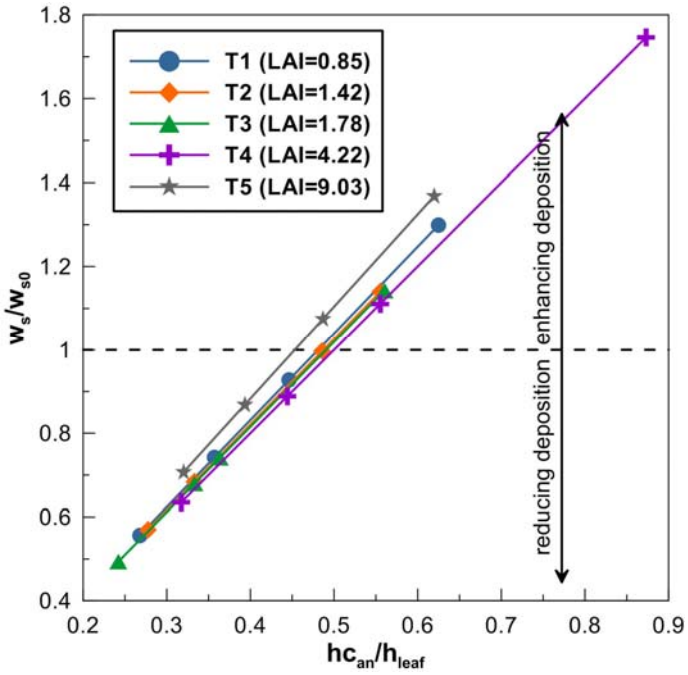

Fig. 5 *Variation of the ws/ws$_0$ ratio to the bending of the canopy (hcan/hleaf) from equation 11, based on the data from the flume deposition tests; the LAI values are noted on the legend, while lower values of the bending ratio correspond to higher flow velocity*

3.2.3 Sediment erosion

Considering the erodibility of the vegetated bed, similar effort was made to relate the erosion fluxes to the characteristics of the dwarf-grass. However, given that the erosion law is highly complex and affected by both the excess shear stress at the bed and sediment/vegetation features, no clear relation was found between the bending of the leafs and the erosion rates measured in the flume. Even though the erosion rates measured in the flume generally increase with stronger inclination of the canopy, a decrease of the bending ratio (h_{can}/h_{leaf}) could not be directly linked to higher erosion fluxes in our numerical experiments. Based on the observations made for the contribution of the canopy to the deposition fluxes, it would be expected that highly bent canopies would produce lower erosion to the bed due to efficient 'protection' of the surface layer and the possible collision and redeposition of freshly eroded matter with the overlying bent leafs. However it is also likely that under strong shear conditions the scraping of leafs with the sediment could induce a form of mechanical erosion that could enhance erosion rates. Given that no safe conclusion can be drawn in the present study, we chose to relate the erosion rates only to the LAI, where a more clear relationship exists. Two important mechanisms were observed: i) excepted T4, all vegetation

experiments showed lower erosion fluxes than the bare mud reference test, which is consistent with the anticipated sediment stabilising effect of the seagrass observed in Ganthy et al., 2013a ii) considering vegetation experiments only, for relatively low LAIs (T1 to T4) the increase of the meadow density causes increase of the erosion fluxes, while for highly dense meadows (T5) the erosion rates are significantly lower.

The following formulations for the erosion parameters were fitted to the data:

$$\tau_{cr,e} = \xi \cdot c^{\zeta} \quad (12)$$

$$\varepsilon = \varepsilon_{bs} \cdot \exp\left(-0.5 \cdot \sqrt{LAI}\right) \quad (13)$$

The critical shear stress coefficients, ξ and ζ, and the erosion rate constant, ε_s , were calibrated at 0.005, 0.5 and 10^{-5}kg/m^2/s, respectively using the bare sediment erosion test (Tsed), and applied to the mud class. As consolidation effects are not accounted for, the erosion critical shear stress for mud is constant. The addition of the term in brackets (exponential function of LAI) is used to express the canopying effect of *Zostera noltei* and the corresponding reduction of erosion rates (in most cases, apart from T4) and applied for all sediment classes. The calibration results from the erosion experiments are presented in the following section.

3.3Ecological modelling and sediment

Suspended particles in the water column affect the growth of *Zostera noltei* due to light scattering and reduction of the available PAR. This impact is taken into account by the model through an appropriate light attenuation function, K (Plus et al., 2003):

$$K = \exp\left(-I_{ext} \cdot d\right) \quad (14)$$

where d is the depth in the water column and I_{ext} is the light extinction coefficient that is calculated taking into account light extinction due to Chla and sediment particles. The full coupling of the model enables the description of the interaction between dwarf-grass growth and suspended sediment (the former changing flow and erosion/deposition rates and the latter changing K and thus the *Zostera notlei* biomass)

4. Results

The flow and turbidity measurements collected during the fume experiments were used to calibrate and validate the modelling approach. The conditions in the laboratory experiments were reproduced using the MARS-3D model and a configuration that allows the recirculation of both flow and sediment fluxes; the dimensions of the channel and of the 'vegetated bed' were set the same as the flume conditions, using a horizontal spacing step of 0.15m and 40 logarithmically distributed sigma layers in the vertical.

4.1 Model Calibration

4.1.1 Calibration of hydrodynamics

The comparison of simulated velocity profiles and the corresponding flume data is given in Figure 6. The simulated values follow the measured profiles very closely, with both the velocity reduction inside the canopy and the increase at the flow-canopy interface to be adequately reproduced by the model. The correlation coefficients calculated are very high, well over 0.9, for all 6 experiments and the Root Mean Square Error (RMSE) ranges from 1 to 4cm/s (Table 2). For the denser meadows the model seems to slightly underestimate the velocity reduction in the upper region of the canopy (exchange zone) and essentially predicting milder velocity gradients at the interface between canopy and flow (e.g. T5 in Fig.6). However, these differences and the overall error are generally small and the description of hydrodynamics by the model is considered very satisfactory.

***Table 2**. Correlation coefficients and RMSE values between flume measurements and model results*

	Tsed	**T1**	**T2**	**T3**	**T4**	**T5**
R^2	0.99	0.95	0.99	0.98	0.95	0.93
RMSE [m/s]	0.009	0.030	0.012	0.015	0.032	0.042

An example of the simulated in the flume for two different meadow densities (test-cases T2 and T4) and the same free-stream velocity (0.3 m/s) are presented in Figure 7. The flow at the wake of the vegetation was also affected, with reduction of the velocities near the bed, compared to the bare sediment, and an upward shift of the local peak velocities due to the deflected flow. Directly upstream from the canopy the velocities are intensified, which is attributed to the transition from boundary-layer flow upstream of the canopy to a mixing-layer type flow within the canopy. This effect was more pronounced in cases of highly dense meadows, due to increase of flow blockage (i.e. T4 versus T2 in Fig.7).

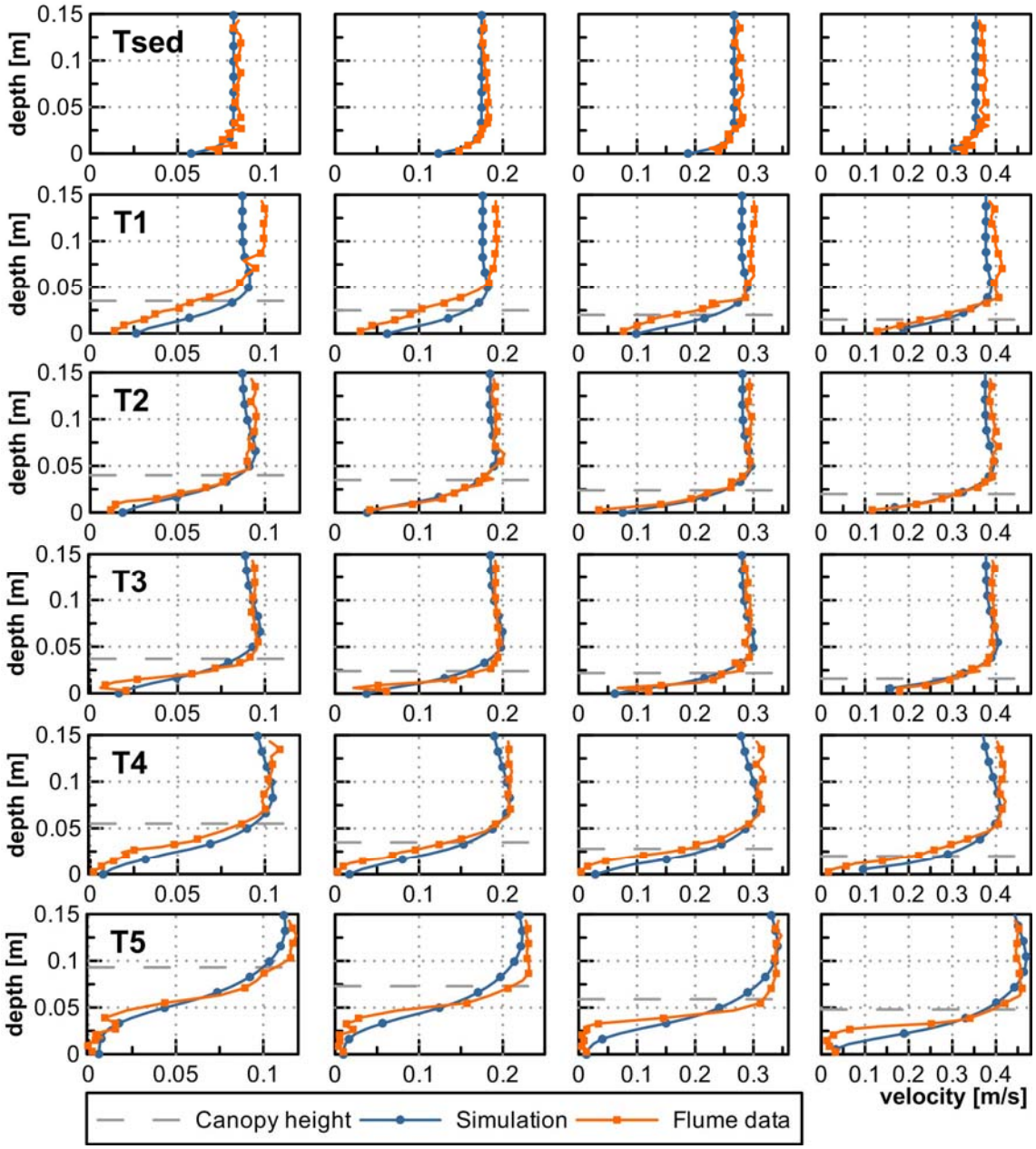

Fig. 6 *Evolution of vertical velocity profiles (for each of the 4 velocity step intervals: 0.1, 0.2, 0.3 and 0.4m/s from left to right) during the laboratory tests (orange lines with squares) with the corresponding simulated profiles (blue lines with circles) for all the tests (from top to bottom: Tsed, T1, T2, T3, T4 and T5). The dashed line denotes the height of the bent canopy at each velocity step*

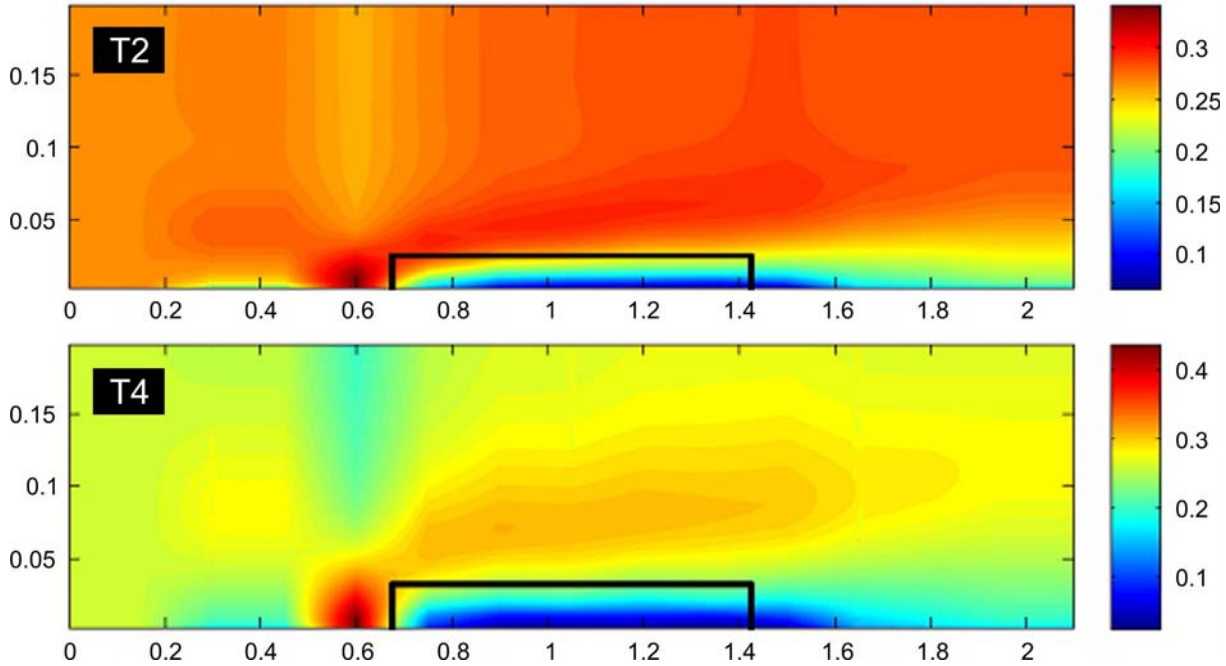

Fig. 7 *Transect of the simulated flume velocities for the T2 (upper panel) and the T4 (lower panel) experiments and for a free-stream velocity of 0.3 m/s; the vegetated area is denoted by a solid black line*

4.1.2 Calibration of erosion/deposition rates

The correlation of simulated and measured time-series of suspended sediment concentrations is presented in Figure 8. The simulated deposition tests generally agree well with the experimental data, apart from a small depreciation of the settling rates near the end of the experiment (low velocities). However, the differences are relatively small and the general agreement of the morphology and deposition rates of the tests are sufficient for the deposition calibration purposes. This can also be noted by the RMSE values presented in Table 3 that are given non-dimensional, so as to follow the graphical representation of the results. The errors are generally small, ranging 2.2 to 8.9%, values and correspond to concentration variability that ranges from 12.6 to 59.6 mg/l.

Table 3*. RMSE for the deposition and erosion tests and for all velocity steps; the former is expressed as percentage and the latter as sediment concentration*

	Vel. step	Tsed	T1	T2	T3	T4	T5
Deposition Tests RMSE [%]	**Ū=0.4m/s**	2.20%	-	4.12%	3.02%	3.30%	2.61%
	Ū=0.3m/s	7.40%	-	3.98%	4.25%	5.60%	4.68%
	Ū=0.2m/s	3.88%	-	4.26%	2.74%	6.60%	5.24%
	Ū=0.1m/s	7.12%	-	5.62%	6.31%	8.57%	8.90%
Erosion Tests RMSE [mg/l]	**Ū=0.1m/s**	2.62	1.65	3.80	2.06	3.48	1.27
	Ū=0.2m/s	2.32	1.40	1.97	1.37	1.87	1.54
	Ū=0.3m/s	1.09	0.71	1.56	1.31	1.20	2.68
	Ū=0.4m/s	2.06	1.69	0.95	2.67	0.79	1.65

The best fit of the simulation to the flume data for the erosion tests is the one depicted in Figure 9. The simulated erosion experiments agree with the mean concentration values of each velocity step, but not with the micro-fluctuations of the values; these fluctuations are most likely due to small-scale shifts in velocities inside the flume, or due to mechanical erosion by the scraping of leaves on the sediment that were not reproduced by the model. Similarly to the deposition tests, the RMSE of the simulations are given in Table 3. Their values are generally low, with the peak error to be of the order of 3.8 mg/l.

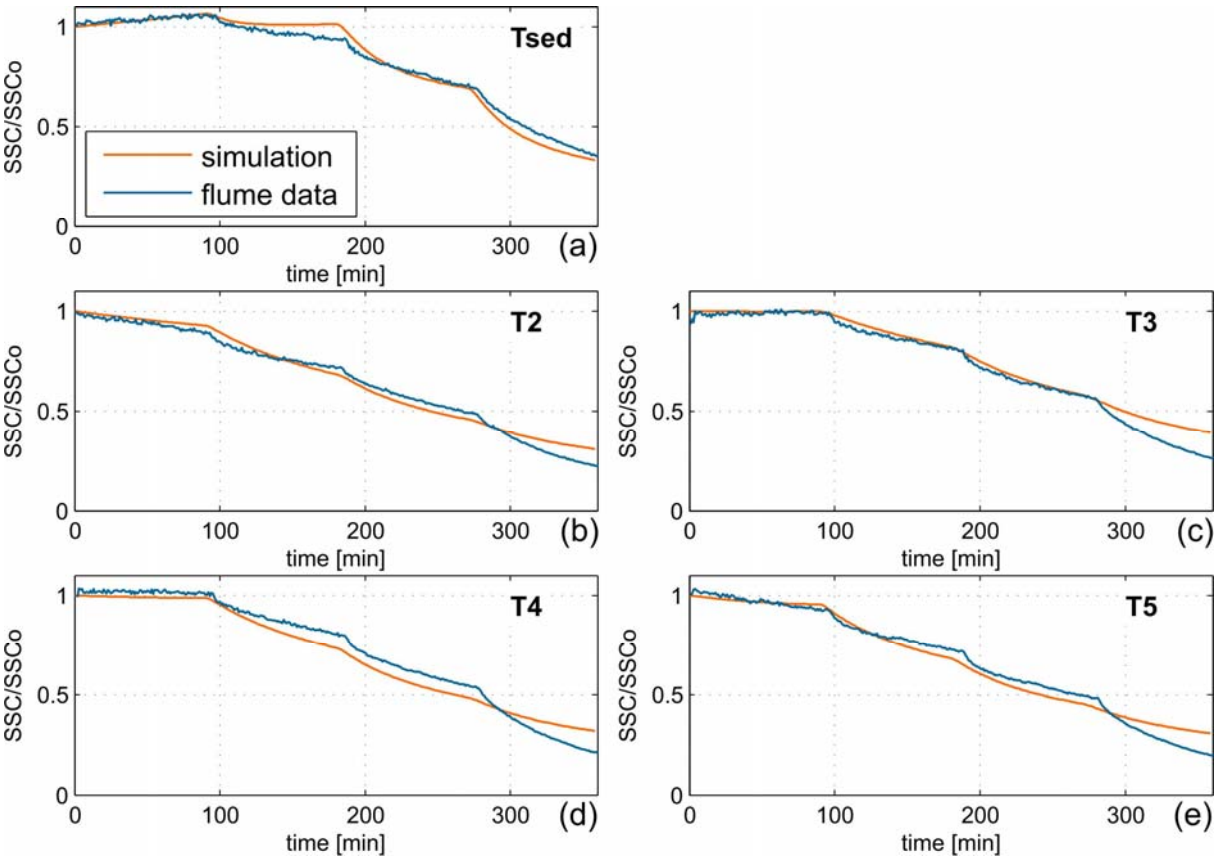

Fig. 8 *Comparison of simulated (orange curve) and experimental (blue curve) deposition tests*

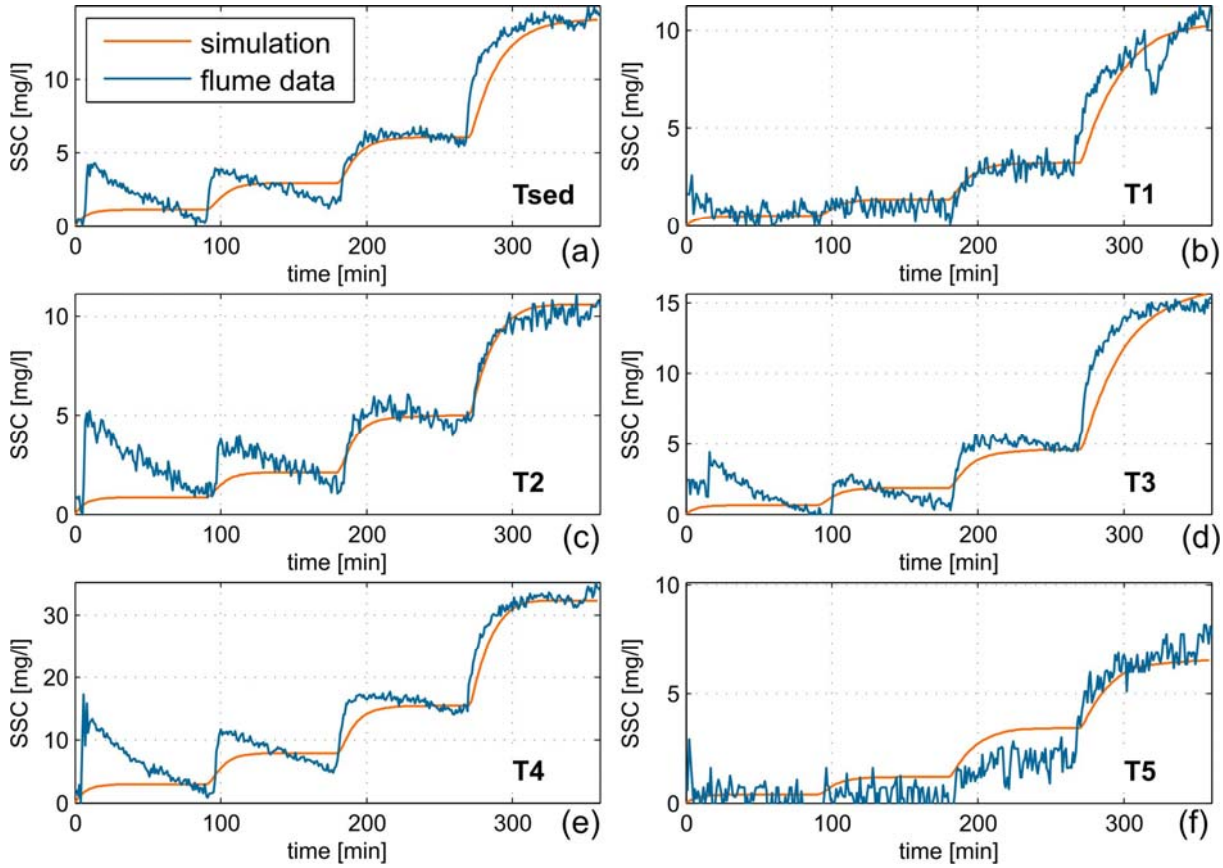

Fig 9 *Comparison of simulated (orange curve) and experimental (blue curve) erosion tests*

4.2 Application in the Arcachon Bay

The model is applied in the Bay of Arcachon in a computational grid that covers the aquatic domain of the lagoon, extending eastwards to longitude -1.46ºE and at latitudes between 44.34 and 44.89ºN (Fig.1) and covering an area of 61.1 x 39.95 km. The bathymetry reaches depths of around 50m at the eastern open boundary. The horizontal discretization step is 235m, 10 sigma layers are used in the vertical inside the water column and another 10 vertical layers are used for the description of the surface (initialized at 1m) sediment of the bed. The input parameters of the coupled model include atmospheric forcing, exchanges at the open boundaries, inflow of freshwater, fine sediments and nutrients (nitrate, phosphate, silicate, and ammonium) from the 7 rivers of the area (Fig.1), while both sediment classes (sand and mud) can enter suspension during bed erosion of the bed. The sand diameter used in the model applications was 0.15 mm, while for the fine fraction the primary aggregates' settling velocity was 0.05 mm/s (diameter of 10 µm). More specifically, the hydrodynamic forcing of the model includes (i) the sea surface elevation (at the boundaries) and (ii) the atmospheric conditions (throughout the domain). Boundary conditions for the sea surface elevation are provided by two nested models of decreasing extensions: 40°N to 65°N and 15°E to 20°W for the largest model and 44.22°N to 45.14°N and 0.87°W to 1.64°W for the intermediate model. All results are presented for the detailed model (Fig.1). Water height variations at the largest model

boundaries are provided by the global hydrodynamics tidal solution FES2004 (Lyard et al. 2006). Realistic atmospheric conditions (air temperature, atmospheric pressure, nebulosity, relative humidity, wind speed and direction) are supplied by the Meteo-France ARPEGE model (Déqué et al. 1994). Biological (*Zostera noltei* shoot densities and biomasses, Ganthy et al. 2013a) and hydrological (SPM, Arcachon Bay Hydrological Network, Ifremer-ARCHYD) field datasets of 2009 were used to compare model results with observations.

Following, results from simulations in the Arcachon Bay are presented and discussed, including investigations of the effects of *Zostera noltei* on hydrodynamics and Suspended Particulate Matter (SPM) concentrations in the domain and the reproduction of dwarf-grass growth by the model. It is noted that the composition of deposited sand and mud obtained after one year hydro-sedimentary simulations (not shown here - used as initial sediment distribution) is in good agreement with corresponding mud and sand content defined after surface sediment or core sampling (Kombiadou et al. 2013), providing a first indication of the effective reproduction of the dominant dynamics in the lagoon by the model.

4.2.1 Effects of Zostera noltei on hydrodynamics

Two simulations were implemented considering different dwarf-grass densities (low: 4000-9000 shoots/m^2 and high: 11000-22000 shoots/m^2) in order to investigate the reproduction of the impacts of the *Zostera noltei* on the local hydrodynamics and to estimate the extent of these effects in the Bay of Arcachon for variable dwarf-grass populations; these densities are representative of winter and summer conditions (Auby and Labourg 1996), thus corresponding to the decay and peak-growth phases of the annual life-cycle of the species in the Bay. The results of these two simulations were compared to the ones obtained from a simulation that did not take into account the presence of vegetation (bare sediment case). Figure 10 presents the relative difference in near-bed velocities for high and low densities of *Zostera noltei* meadows, with reference to the bare sediment case; the values are averaged over four tidal periods that correspond to spring tidal conditions in the bay. It can be noted that velocities are reduced by a local maximum of 60% for the high density period (Fig.10c, typical of summer conditions), while the average reduction in the western, highly vegetated, areas is of the order of 20-50%; the attenuation in the eastern area is lower, ranging from 10 to 30%. As anticipated, the corresponding results for the low density period (Fig.3d, typical of winter conditions) have similar spatial distribution, but significantly lower velocity attenuation that reaches a local maximum of 35%. The reduction of near-bed velocities implies related reduction to the bottom shear stress and thus is expected to induce higher deposition and lower resuspension/erosion rates at the locations of dwarf-grass presence. Following, results from applications of the coupled model in the domain of Arcachon are presented and discussed.

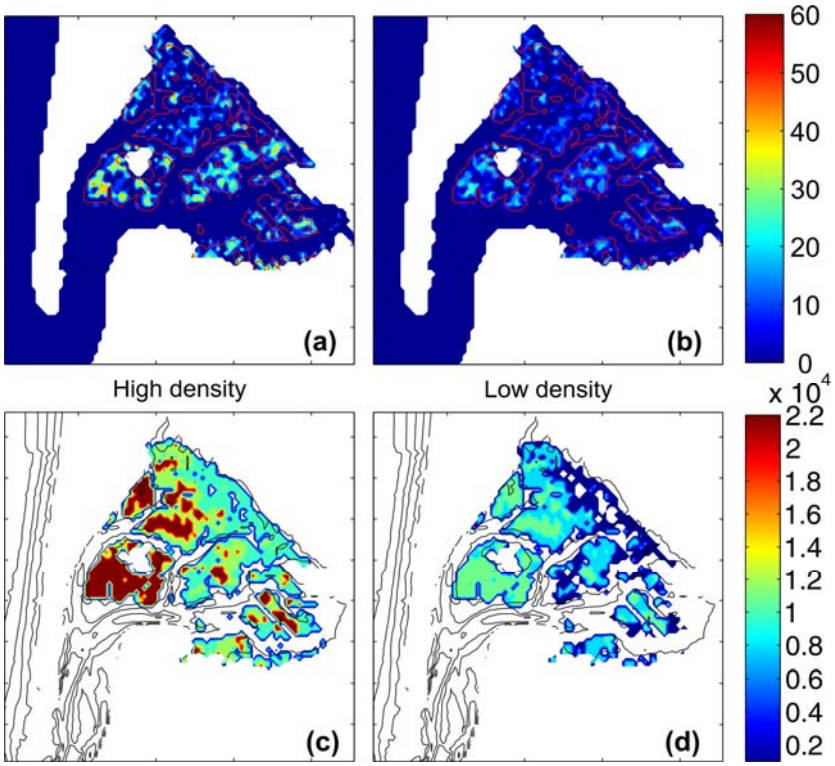

Fig. 10 *Attenuation of near-bed velocity [%] (a and b) in the presence of high and low density meadows [shoots/m^2] (c and d, respectively); the curve denotes the vegetated areas, while the attenuation values are time-averaged over four tidal cycles*

4.2.2 Effects of Zostera noltei on SPM concentrations

In the present section, we present results from applications of the fully coupled model in the Arcachon bay and, thus, correspond to the 'natural realistic' conditions, as observed in the field. As described previously, the presence of *Zostera noltei* affects the local flow and sediment fluxes, SPM is affected by the presence of seagrass and the growth of the seagrass is determined by the flow conditions, nutrient and light availability, the latter controlled by the suspended sediment concentrations. Suspended sediment concentrations are compared with corresponding measurements collected by the Arcachon Bay Hydrological (Archyd) network (Ifremer) at characteristic stations. Figure 11 shows the correlation of field data with two different simulations for the year of 2009 and at four stations in the bay (their location is noted in Fig.1): two in the inner part (Jacquets and Comprian) and two at the entrance of the bay (Buoy07 and Buoy13). These simulations consider different values for the maximum settling velocities predicted by the model for the fine sediment fraction, with the one to take into account twice the maximum settling velocity of the other (2 mm/s and 1 mm/s); we used the following naming convention for these simulations: High Settling Velocity (HSV, considering 2 mm/s as a peak settling rate) and Low Settling Velocity (LSV, considering 1 mm/s as a peak settling rate). It can be noted that for Jacquets the correlation with the measurements is better for LSV, while HSV significantly depreciates SPM (RMSE 3.49 mg/l and 3.58 mg/l, respectively). For the Comprian station, however, LSV predicts higher SPM concentrations than the ones measured in the field, while HSV seems to approximate these measurements more accurately (RMSE 7.41 mg/l and

5.37 mg/l, respectively); a general observation regarding all stations is that HSV predicts very low (nearly zero) concentrations at low tidal velocities, while LSV improves the 'floor' SPM values significantly, but, at the same time, produces peak concentrations well over the measured ones. However, it should be noted that the Archyd measurements are conducted at low or high tide, thus when tidal currents are the weakest. Therefore, the field measurements do not depict sediment dynamics at maximum tidal energy. For the two stations at the entrance of the bay, LSV provides results that are closer to the *in situ* recordings, with RMSE of the order of 5.44 mg/l and 2.30 mg/l for Buoy07 and Buoy13 (versus 6.94 mg/l and 4.60 mg/l for the HSV run); however, for Buoy07 the decrease in settling velocities did not change SPM concentrations significantly. This is probably due to location of the station, combined with the dominant circulation patterns in the bay, analysed further in the discussion section.

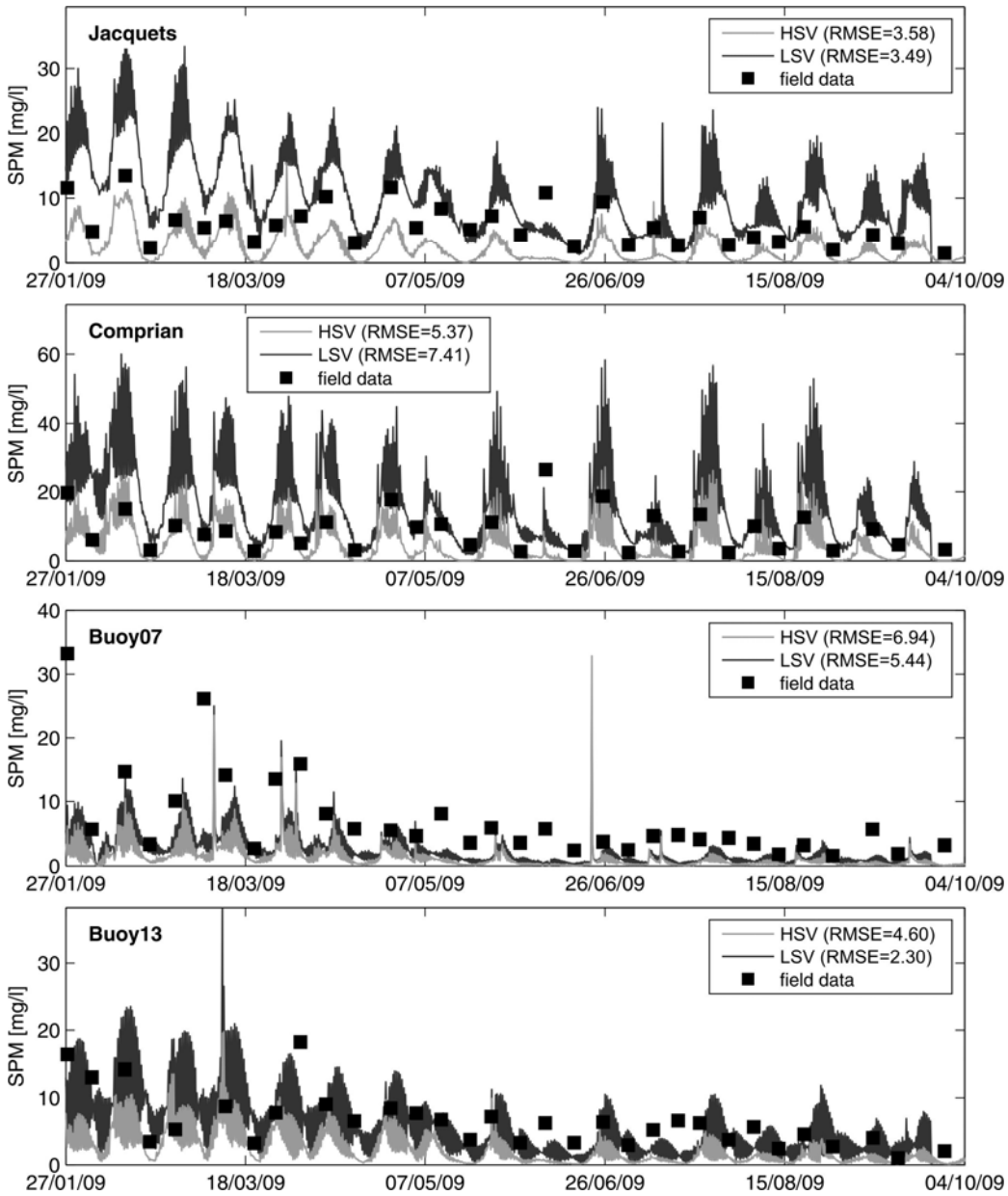

Fig. 11 *Comparison of SPM concentrations in four stations in the Arcachon lagoon (Fig.1) simulated using two different sediment characteristics (curves) and data from in situ measurements from the Archyd network (squares)*

To investigate the effect of the dwarf-grass on the SPM in the lagoon of Arcachon we compare two different simulations: one with the Presence of Vegetation (PV = HSV) and one in the Absence of Vegetation (AV). More specifically, the PV simulation was performed using the fully coupled model, thus considering the effects of dwarf-grass to the hydro and sediment dynamics and the life cycles of the *Zostera noltei* from the biogeochemical cycles, described in the previous chapter. On the other hand, the AV simulation took into account only the hydro-sediment dynamics, completely disregarding the presence of dwarf-grass. These simulations considered the settling scenario of HSV. The comparison of the two cases is presented in Figure 12 for three locations in the bay (Fig.1): location 1 inside the vegetated area, location 2 in a medium depth, unvegetated area of the mudflats and location 3 in a deep channel area near the entrance of the inner bay. The model works well in terms of reproducing the retention of sediment by the vegetation due to the combined canopying and hydrodynamic damping effects. The reduction of SPM inside the meadow (Fig.12a) is significant and reaches 30-65% at peak tidal velocities, whereas at low/high tide the effect is negligible. At the same time, the two simulations show minor differences in shallow areas unoccupied by dwarf-grass (Fig.12b) and, therefore, the model does not overestimate the effects and the changes to suspended sediment dynamics predicted by the model are indeed solely due to the presence of vegetation. The differences in SPM concentrations near the entrance of the bay (Fig.12c) are due to the changes in suspended sediment in the bay between the 2 simulations, directly caused by the presence of meadows on the intertidal flats. The lower SPM inside the meadows in PV, compared to AV, causes a general decrease of SPM in the bay; this reduction of sediment in suspension also appears in location 3 for the PV case, due the sediment flushing from the lagoon to the open sea through the deep and highly energetic channels in the bay. No clear impact of the seasonal *Zostera noltei* growth parameters can be distinguished in the results of the vegetated area; this is most likely due to the seasonal atmospheric forcing combined with the annual unimodal pattern of dwarf-grass growth. During winter the wind-driven circulation is stronger and *Zostera noltei* density and LAI are low, while the opposite is true for summer conditions. High velocities cause flexible leafs to bend and, thus, lead to more profound canopying effects, which, even though the meadows are sparse, are quite effective in retaining sediment. Contrastingly, low velocities produce less bending to the canopy, but, at the same time, coincide with highly developed meadows that produce higher damping to the near-bed hydrodynamics. Generally, the results from the large-scale application of the model are in agreement with the theoretical background and literature reviews (Fonseca and Fisher 1986; Gacia et al. 1999; Thompson et al. 2004), and show that the model reproduces the impact of aquatic vegetation on sediment transport effectively. The strong reduction of SPM levels also indicates the high significance of the dwarf-grass meadows on the sediment dynamics in the bay of Arcachon.

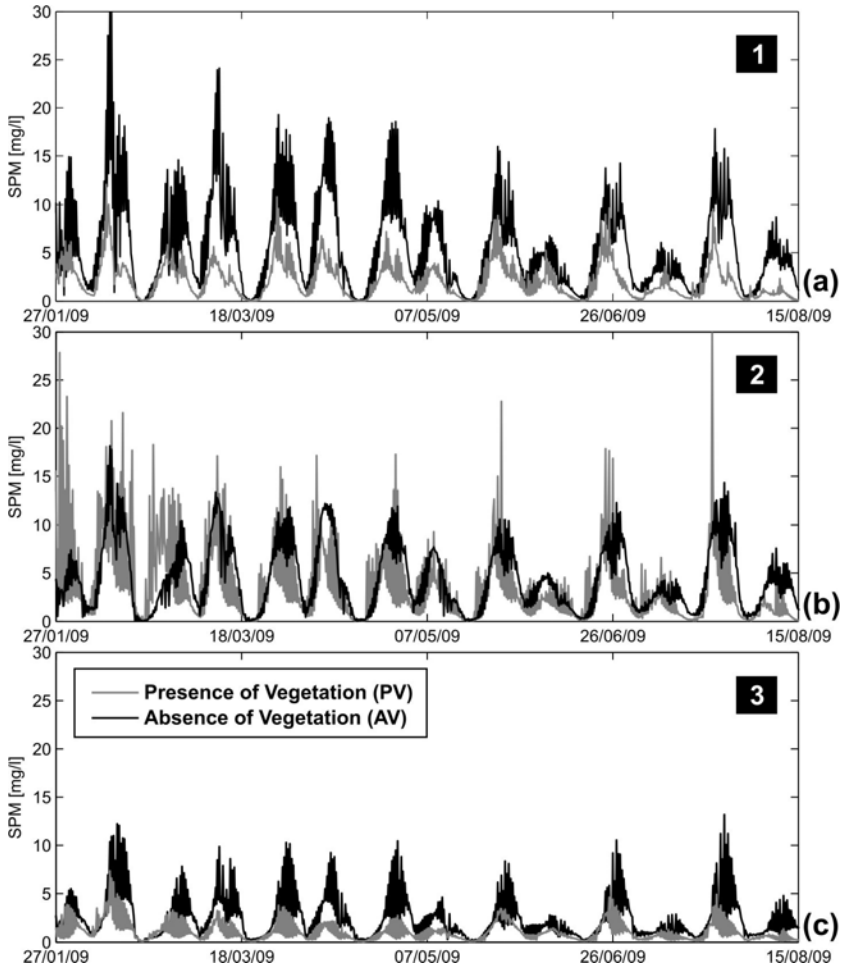

Fig. 12 *Comparison of SPM concentrations in three locations in the Arcachon lagoon (1, 2 and 3 in Fig.1, shown in a, b and c, respectively) from two simulations, one including the Presence of Vegetation (PV) and one that considers Absence of Vegetation (AV)*

4.2.3 Zostera noltei growth

Regarding the reproduction of the dwarf-grass growth by the model, a comparison of simulated time-series of density and leaf biomass and corresponding values measured in the field (Ganthy et al. 2013a) near location 1 is depicted in Figure 13. The correlation of both parameters with the field observations is satisfactory, with the simulated values to approximate the measurements adequately, both in terms of values and curve morphology. The model reproduces the life cycles of *Zostera noltei* accurately, with the peak in seagrass density to appear around the end of August and the corresponding peak in leaf biomass to follow one month later (end of September), periods that agree with related observations from the Arcachon lagoon. It is noted that results for other biological parameters (not shown here) also agree well with corresponding field measurements (Auby and Labourg 1996).

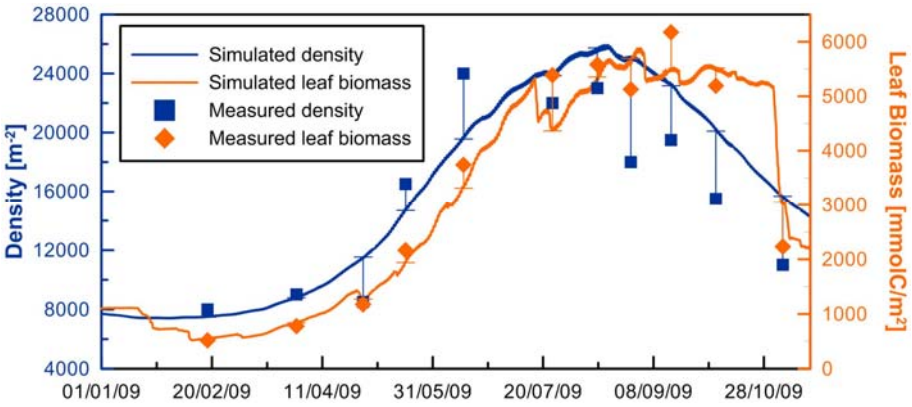

Fig. 13 *Evolution of simulated (curves) and measured (points) Zostera noltei density (corresponding to left axis) and leaf biomass (corresponding to right axis)*

5. Discussion

The model parameters regarding the effects of *Zostera noltei* on the local hydrodynamics and the deposition and erosion rates were calibrated using flume experiments. Regarding hydrodynamics, the simulations showed an increase of the velocities at the canopy-flow interface and a growth of the shear layer downstream the leading edge of the canopy, observations that are in accordance with analogous flume experiments (e.g. Rominger and Nepf 2011). The reproduction of the flume velocity profiles by the model was good, with a generally low root mean square error that ranged from 9 to 42 mm/s for the tested range of flow velocities (0.1 to 0.4 m/s, respectively). The flow at the wake of the vegetation was also affected, with reduction of the velocities near the bed compared to the bare sediment and an upward shift of the local peak velocities due to the deflected flow. Directly upstream from the canopy the velocities are intensified, due to the transition from boundary-layer flow upstream of the canopy to a mixing-layer type flow within the canopy, effect that was more pronounced for highly dense meadows due to increased flow blockage; such features have been reported from similar flume experiments (e.g. Gambi et al. 2001; Rominger and Nepf 2011) and were also reproduced by the model (Fig.8). As for the settling rates and erodibility of the sediment, the simulated deposition and erosion experiments fit well with the corresponding flume recordings.

The investigation regarding the sediment dynamics in the bay and the correlation between simulation and field observations (Fig.11) showed that the modelling results are sensitive to the values assigned to sediment settling velocities; setting relatively high settling rates to the fine sediment fraction produced results that generally compared well with corresponding field measurements, but with nearly zero concentrations during slack water, which contradicts our knowledge on the conditions in the field. On the other hand, decreasing settling was effective in terms of improving the lowest concentrations predicted by the model, but the corresponding peaks were well over the ones recorded by the Archyd network. However, given that the Archyd measurements are not conducted at maximum tidal circulation the actual

maximum concentrations in the bay could be higher than the ones recorded by the network, supposition that is supported by high-frequency measurements. An example of hourly SPM recordings (Paolin 2012) during one tidal cycle for the station of Comprian is shown in figure 14. These data show that the peak SPM concentrations in Comprian can be 6 times greater than the lowest ones (30mg/l versus 5mg/l, respectively) during one typical cycle. In any case, the settling velocities considered by the model should and will be fine-tuned further, if possible using field data at high frequency.

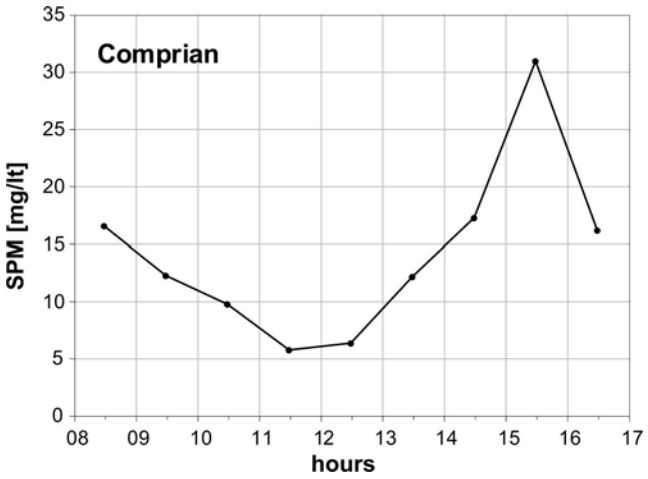

Fig. 14 *Variation of SPM [mg/l] in the station of Comprian during one tidal cycle (adapted from Paolin 2012). The measurement was conducted on May 11th, 2012 and the high and low tidal levels correspond to 10:21 and 16:11, respectively*

The reduction of the settling velocity did not have the same impact on SPM at the two stations near the entrance of the bay. The differences between HSV and LSV were significant for Buoy13, whereas for Buoy07 the two simulations provided similar results. This is probably due to location of the stations, combined with the dominant circulation patterns in the bay and the morphology of the entrance; two channels that are separated by the Arguin bank (Fig.1) allow the communication of the bay with the open sea. At the same time, the residual circulation within the entrance of the lagoon is directed outwards (from the bay to the open sea) along Cape Ferret (Fig.1), while the residual fluxes are directed inwards along the Pyla coast (Plus et al. 2009). The ebb-dominated flow in the area is expected to lead suspended matter to exit the lagoon primarily through the westernmost channel (near Cape Ferret) of the opening. Thus, in cases of elevated SPM in the bay (LSV) we would expect higher concentrations along cape Ferret (due to circulation that transports matter from the inner part) than along the Pyla coast. This outflow pattern, which is also supported by the findings of Cayocca (2001), is the most likely reason for the small differences in SPM between the two simulations in Buoy07.

The comparison of the two simulations with and without the presence of *Zostera noltei* (PV and AV, respectively) shows that the coupled model is successful in simulating sediment retention in the vegetated areas of the bay (Fig.12), both in periods of growth and degeneration of the dwarf-grasses (Ganthy et al. 2013a). This effect was only observed inside the meadow, with a peak reduction in SPM of the order of

65%, whereas in the unvegetated mudflats the inclusion of the seagrasses practically had no impact on the modelling results. It is important to highlight that the presence of vegetation had a strong impact on SPM throughout the year, even though during winter when the degeneration of *Zostera noltei* and the increased wind forcing would be expected to increase the erodibility of sediment, compared to the low-energy and high meadow density summer period.

Regarding the biological parameters, the simulations provided very satisfactory results (Fig.13); especially for the growth of the dwarf-grasses in the bay, the model reproduces the annual unimodal pattern of *Zostera noltei* growth and decay in the Arcachon Bay (Auby and Labourg 1996; Ganthy 2011).

Conclusions

The present paper focused on the development of a 3D numerical model simulating the interactions between hydrodynamics, sediment transport and biological parameters in the presence of *Zostera noltei* meadows and the presentation of preliminary modelling results from the Bay of Arcachon. The three-dimensional model was successfully coupled since the changes to the local flow conditions due to the interference of the flexible seagrass blades directly feed both the sediment transport modules and the biological cycles in the domain. At the same time, information regarding the suspended matter in the water column is linked to the primary productivity and to the growth of the dwarf-grass themselves, through changes to the light attenuation in the column. Simulated meadow characteristics (leaf height and density) provide direct feedback to the hydrodynamic modules.

Investigation of the impact of different dwarf-grass densities to the near-bed flow in the bay showed that during peak growth of the meadows the average reduction to the local velocities is of the order of 20-50%, while during degradation the changes are significantly lower, ranging between 10 and 20% on average. Simulated SPM concentrations in the bay were generally comparable with field measurements from the Archyd network. Comparing the results of the coupled model with corresponding results with no effect of vegetation showed that the changes in SPM simulated by the model are concentrated almost exclusively in areas populated by dwarf-grasses.

The final objective of the work is to apply the model to validate/disprove possible scenarios (e.g. changes in sediment/nutrient influxes) for the reduction in *Zostera noltei* coverage observed during the last decades in the lagoon. The coupled model will also be used for the investigation of scenarios regarding extreme hydro-meteorological conditions and their impacts on the spatial distribution of dwarf-grass and the related changes to the turbidity in the field. The preliminary results are encouraging regarding the effectiveness of the model to simulate the complex balance and interrelationship between hydrodynamic, sediment and biological parameters' dynamics in the Bay of Arcachon and provide the basis for the further development and future applications of the model.

Acknowledgements

The work presented was funded by SIBA (Syndicat Intercommunal du Bassin d'Arcachon) and IFREMER (Institut Français de Recherche pour l'Exploitation de la Mer) and partly by the French Research National Agency program ANR IZOFLUX. The authors wish to thank Isabelle Auby and Mélina Paolin (IFREMER) for kindly permitting the reproduction of field measurements from the Arcachon lagoon.

References

Ackerman JD, Okubo A (1993) Reduced Mixing in a Marine Macrophyte Canopy. Funct Ecol 7(3): 305-309

Auby I, Labourg P-J (1996) Seasonal dynamics of *Zostera noltii* hornem. in the Bay of Arcachon (France). J Sea Res 35(4): 269-277

Backhaus JO, Verduin JJ (2008) Simulating the interaction of seagrasses with their ambient flow. Estuar Coast Shelf Sci 80: 563–572

Bouma TJ, De Vries MB, Low E, Kusters L, Herman PMJ, Tánczos IC, Temmerman S, Hesselink A, Meire P, van Regenmortel S (2005a) Flow hydrodynamics on a mudflat and in salt marsh vegetation: identifying general relationships for habitat characterisations. Hydrobiol 540: 259–274

Bouma TJ, De Vries MB, Low E, Peralta G, Tánczos IC, van de Koppel J, Herman PMJ (2005b) Trade-offs related to ecosystem engineering: A case study on stiffness of emerging macrophytes. Ecol 86(8): 2187–2199

Bouma TJ, Friedrichs M, Klaassen P, van Wesenbeeck BK, Brun FG (2009) Effects of shoot stiffness, shoot size and current velocity on scouring sediment from around seedlings and propagules. Mar Ecol Prog Ser 388: 293–297

Cayocca F (2001) Long-term morphological modeling of a tidal inlet: the Arcachon Basin, France. Coast Eng 42: 115–142

Cholvy J.P. (2008) Quantifier et qualifier la fréquentation touristique du Bassin d'Arcachon. Rapport SIBA (in French)

Dauby P, Bale AJ, Bloomer N, Canon C, Ling RD, Norro A, Robertson JE, Simon A, Théate JM, Watson AJ, Frankignoulle M (1995) Particle fluxes over a Mediterranean seagrass bed: a one year case study. Mar Ecol Prog Ser 126: 233-246

Defina A, Bixio AC (2005) Mean flow and turbulence in vegetated open channel flow. Water Resour Res 41: W07006. doi:10.1029/2004WR003475

Déqué M., Dreveton C., Braun A., Cariolle D. (1994) The ARPEGE-IFS atmosphere model: a contribution to the French community climate modelling. Climate Dyn 10: 249-266

Fabrègues L. (2005) Arcachon, l'année des records. Le Marin - hors série - Ports de pêche, avril 2005 (in French)

Fischer-Antze T, Stoesser T, Bates P, Olsen NRB (2001) 3D numerical modelling of open-channel flow with submerged vegetation. J Hydraul Res 39(3): 303-310

Fonseca MS, Fisher JS (1986) A comparison of canopy friction and sediment movement between four species of seagrass with reference to their ecology and restoration. Mar Ecol Prog Ser 29:15–22

Fonseca MS, Koehl MAR (2006) Flow in seagrass canopies: The influence of patch width. Estuar Coast Shelf Sci 67: 1-9

Gacia E, Granata TC, Duarte CM (1999) An approach to measurement of particle flux and sediment retention within seagrass (*Posidonia oceanica*) meadows. Aquat Bot 65(1-4): 255-268

Gambi MC, Nowell AR, Jumars PA (1990) Flume observations on flow dynamics in *Zostera marina* (eelgrass) beds. Mar Ecol Prog Ser 61: 159–169

Ganthy F, Verney R, Sottolichio A (2013a) Seasonal modification of tidal flat sediment dynamics by seagrass meadows of *Zostera noltii* (Bassin d'Arcachon, France). J Mar Syst 109–110: S233-S240

Ganthy F, Verney R, Sottolichio A (2013b) A numerical investigation on the effects of small and flexible seagrass *Zostera noltii* on water flow. Proc Coast Dyn 2013: 705-716

Ganthy F (2011) Rôle des herbiers de zostères (*Zostera noltii*) sur la dynamique sédimentaire du Bassin d'Arcachon. Dissertation, University of Bordeaux

Ghisalberti M, Nepf H (2002) Mixing layers and coherent structures in vegetated aquatic flow. J Geophys Res 107(C2): 1-11

Ghisalberti M, Nepf H (2006) The Structure of the Shear Layer in Flows Over Rigid and Flexible Canopies. Environ Fluid Mech 6: 277–301.

Ghisalberti M, Nepf H (2009) Shallow Flows Over a Permeable Medium: The Hydrodynamics of Submerged Aquatic Canopies. Transp Porous Media 78:309–326

Grizzle RE, Short FT, Newell CR, Hoven H, Kindblom L (1996) Hydrodynamically induced synchronous waving of seagrasses: 'monami' and its possible effects on larval mussel settlement. J Exp Marine Biol Ecol 206: 165-177

Guillaud J-F, Andrieux F, Ménesguen A (2000) Biogeochemical modelling in the Bay of Seine (France): an improvement by introducing phosphorus in nutrient cycles. J Mar Syst 25: 369-386

Henocque Y. (2003) Development of process indicators for coastal zone management assessment in France. Ocean & Coastal Management 46 (3-4): 363-379

Huret M, Sourisseau M, Petitgas P, Struski C, Léger F, Lazure P (2013) A multi-decadal hindcast of a physical–biogeochemical model and derived oceanographic indices in the Bay of Biscay. J Mar Syst 109–110: S77–S94

Kombiadou K, Verney R, Plus M, Ganthy F (2013) Développement d'un modèle intégré pour le Bassin d'Arcachon. Dynamique sédimentaire en lien avec la dynamique des herbiers de zostères. Final Report, Ifremer (in French)

Lazure P, Dumas F (2008) An external-internal mode coupling for a 3D hydrodynamical model for applications at regional scale (MARS). Adv Water Resour 31: 233–250

Le Berre S., Franz T., Brigand L. (2009) Etude de la fréquentation nautique du bassin d'Arcachon - Premiers résultats quantitatifs et cahier des charges méthodologique. Rapport intermédiaire. Direction régionale des affaires maritimes, Aquitaine - service départemental Arcachon - Géomer, UMR 6554 LETG - Université de Bretagne Occidentale (in French)

Le Hir P, Cayocca F, Waeles B (2011) Dynamics of sand and mud mixtures: A multiprocess-based modelling strategy. Cont Shelf Res 31: S135–S149

Lefebvre A, Thompson CEL, Amos CL (2010) Influence of *Zostera marina* canopies on unidirectional flow, hydraulic roughness and sediment movement. Cont Shelf Res 30: 1783–1794

Lopez F, Garcia M (2001) Mean Flow and Turbulence Structure of Open-Chanel Flow through Non-Emergent Vegetation. J Hydraul Eng 127: 392-402.

Lyard F., Lefèvre F., Letellier T, Francis O. (2006) Modelling the global ocean tides: a modern insight from FES2004. Ocean Dyn 56: 394-415

Milbradt P, Schonert T (2008) Eco-hydraulic simulation in coastal engineering. J Hydroinformatics 10-3: 201-214

Nepf H, Ghisalberti M (2008) Flow and transport in channels with submerged vegetation. Acta Geophys 56(3): 753-777

Nepf HM, Vivoni ER (2000) Flow structure in depth-limited vegetated flow. J Geophys Res 105C12: 28547-28557

Neumeier U, Amos CL (2006) The influence of vegetation on turbulence and flow velocities in European salt-marshes. Sedimentol 53: 259–277

Orvain F., Le Hir P., Sauriau P.-G. (2003) A model of fluff layer erosion and subsequent bed erosion in the presence of the bioturbator, *Hydrobia ulvae*. J Mar Res 61: 823-851

Paolin M (2012) Etudes des facteurs contrôlant l'atténuation lumineuse dans une lagune semi-fermée. Calibration d'un modèle bio-optique pour le Bassin d'Arcachon. Technical Report, Ifremer (in French)

Plus M, Dalloyau S, Trut G, Auby I, de Montaudouin X, Emery E, Noël C, Viala C (2010) Long-term evolution (1988–2008) of *Zostera spp.* meadows in Arcachon Bay (Bay of Biscay). Estuar Coast Shelf Sci 87: 357–366

Plus M, Dumas F, Stanisiére J-Y, Maurer D (2009) Hydrodynamic characterization of the Arcachon Bay, using model-derived descriptors. Cont Shelf Res 29: 1008–1013

Plus M, Chapelle A, Ménesguen A, Deslous-Paoli J-M, Auby I (2003) Modelling seasonal dynamics of biomasses and nitrogen contents in a seagrass meadow (*Zostera noltii* Hornem.): application to the Thau lagoon (French Mediterranean coast). Ecol Model 161(3): 213-238

Righetti M, Armanini A (2002) Flow resistance in open channel flows with sparsely distributed bushes. J Hydrol 269: 55–64

Rominger JT, Nepf HM (2011) Flow adjustment and interior flow associated with a rectangular porous obstruction. J Fluid Mech 680: 636–659

Scourzic T., Loyen M., Fabre E., Tessier A., Dalias N., Trut G., Maurer D., Simmonet B (2011) Evaluation du stock d'huîtres sauvages et en élevage dans le Bassin d'Arcachon. Contrat Agence des Aires Marines Protégées & OCEANIDE, 63p.

Temmerman S, Bouma TJ, Govers G, Wang ZB, De Vries MB, Herman PMJ (2005) Impact of vegetation on flow routing and sedimentation patterns: Three-dimensional modelling for a tidal marsh. J Geophys Res 110: F04019. doi:10.1029/2005JF000301

Thompson CEL, Amos CL, Umgiesser G (2004) A comparison between fluid shear stress reduction by halophytic plants in Venice Lagoon, Italy and Rustico Bay, Canada-analyses of in situ measurements. J Mar Syst 51(1-4): 293-308

Verduin, J.J., Backhaus, J.O. (2000) Dynamics of plant-flow interactions for the seagrass *Amphibolis antartica*: field observations and model simulations. Estuar Coast Shelf Sci 50: 185-204.

Widdows J., Pope N.D., Brinsley M.D., Asmus H., Asmus R.M. (2008) Effects of seagrass beds (*Zostera noltii* and *Z. marina*) on near-bed hydrodynamics and sediment resuspension. Mar Ecol Prog Ser 358: 125-126